Proceedings of Meetings on Acoustics

Volume 39 http://acousticalsociety.org/

178th Meeting of the Acoustical Society of America

San Diego, CA

2-6 December 2019

Signal Processing in Acoustics: Paper 1pSP3

An investigation into the performance limitations of active acoustic cloaking using an acoustic quiet-zone

Charlie House, Jordan Cheer and Steve Daley

Institute of Sound & Vibration Research, University of Southampton, Southampton, Hampshire, SO167BA, UNITED KINGDOM; c.house@soton.ac.uk; j.cheer@soton.ac.uk,; s.daley@soton.ac.uk

The use of active control to acoustically cloak an object has been demonstrated previously, and is effective if the scattered component of the pressure field can be measured and directly minimised. In practice, this is non-trivial as a pressure sensor in the sound-field will detect the superposition of the incident and scattered pressures. An alternative approach has been proposed in the literature, using high-order multipole sources to generate a zone of quiet around the scattering object, whilst not radiating into the far-field. This approach performs well, however the use of high-order multipole sources is infeasible for a practical implementation. This paper will explore the limitations of the quiet-zone acoustic cloaking strategy on simulated data of a rigid spherical scattering object, using a practical arrangement of monopole control sources and error sensors. The same arrangement of sources and sensors is also used to directly minimise the scattered sound field, and the two approaches are compared in terms of practicality, control-effort, and performance.

1. INTRODUCTION

The concept of acoustic cloaking has been thoroughly discussed in the literature, as the ability to acoustically conceal an object, such that the sound-field with the object present is identical to that without the object present, has significant benefits for both research and engineering. Passive acoustic cloaks, made of metamaterials consisting of sub-wavelength cells, have been demonstrated successfully in both simulation [1, 2, 3, 4] and experimental [5, 6, 7, 8] domains. However, these passive approaches have seen limited practical application due to their narrow band-gap performance [9]. Active acoustic cloaking methods have also been investigated, enabling much larger bandwidths of control when compared to passive methods and often providing a cloaking strategy that is significantly more robust to variations in the incident field; especially when an adaptive algorithm is used [10]. Active acoustic cloaking systems have been demonstrated successfully in the simulation domain [11, 12, 13], however, practical implementations are more limited as most active acoustic cloaking systems require real-time knowledge of the scattered acoustic field. Various methods of estimating the scattered acoustic pressure from a measurable quantity have been presented in the literature; for example, by using a Virtual Sensing strategy [14], by using analytical or numerical modelling [15, 16], or by using a wave decomposition approach [17].

An alternative approach to attempting to directly control the scattered acoustic pressure was initially presented by Vasquez et al [18, 19], which uses active control to generate a zone of silence around the scattering object. By reducing the incident acoustic wave, the scattered acoustic pressure is also reduced without the requirement of unrealistic a priori knowledge about the scattering object. For this approach to work, the quiet-zone control sources must self-cancel in the far-field to prevent them from influencing the far-field pressure. Therefore, high-order multipole sources [20] were used to generate complex pressure fields with limited numbers of sources. Significant analytical research has been conducted into the formulations for the optimal multipole amplitudes to achieve a quiet-zone whilst enforcing a constraint on the far-field radiation [18, 21, 22], and theoretical investigations into the performance of two-dimensional quiet-zone cloaking systems have also been presented [23, 24, 25, 26].

Whilst these publications provide insight into the potential performance and limitations of a quiet-zone cloaking system, the use of high-order multipole sources limits their practicability; hence, no experimental validations have been published to-date. Using the Kirchoff-Helmholtz Integral [27] to express the high-order multipole sources as a continuous distribution of monopole and dipole sources may give further insight into the source strength distribution. However, this is equally as impractical for a real-world implementation, as continuous distributions of sources are clearly unrealisable. This paper will use simulated data to implement the quiet-zone acoustic cloaking method using a practical arrangement of pressure sensors and a dual-layer array of discrete monopole control sources to acoustically cloak a rigid sphere. The acoustic scattered field will also be directly controlled, as discussed by Cheer [12], and the performance, control effort, and practicalities of both strategies will be compared. This will provide insight into the potential performance of using the quiet-zone control approach to acoustically cloak an object with a practical arrangement of sensors and sources.

Section 2 will outline the modelling environment; providing details of the simulation method as well as the geometry of the scattering object and the arrangement of the control sources and error sensors. The control strategies will be detailed in Section 3 and formulations for the optimal source strengths for both the quiet-zone cloaking method and the direct-minimisation cloaking method will be derived. Section 4 will compare the performance of the two control strategies, and will investigate the required control effort in each case, and Section 5 will provide conclusions and a brief comment on the real-world practicability of both systems.

2. MODELLING ENVIRONMENT

In order to investigate the practical limits on the performance of the quiet-zone cloaking strategy, and to compare the performance to a direct-minimisation approach, a numerical model has been developed using COMSOL Multiphysics. The Boundary Element Method was used to model a rigid spherical scatterer with a radius of $r = 150$ mm, impinged upon by an incident acoustic plane wave. A helical array of 16 acoustic pressure sensors was included in the near-field of the scatterer to measure the acoustic pressure in the quiet-zone, and a circular array of 40 acoustic pressure sensors was implemented in the far-field to measure the far-field scattering, as shown in Figure 1. A dual-layer arrangement of two rings of 16 monopole control sources, which will be used to generate the control field, were arranged around the scattering object, oriented to point radially, and spaced 0.11 m apart.

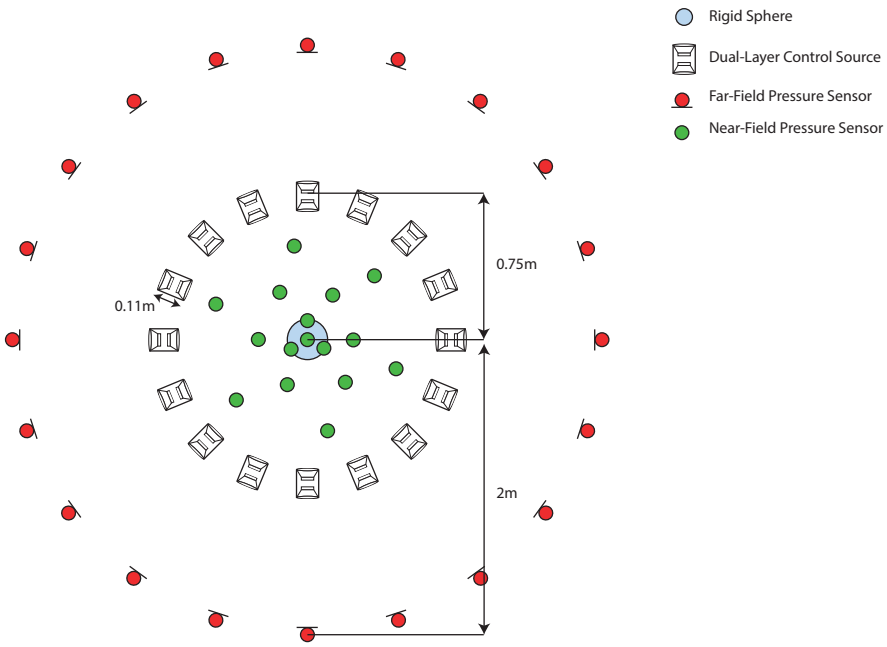

Figure 1: A schematic diagram showing the location of the scattering object and the source and sensor arrays.

A numerical model was chosen, in this case, over an analytical model as it enables more complex features to be included, which would allow the model to more closely match a practical setup. For example, the control sources could be modelled as rigid cylinders with an imposed velocity on their caps, or the performance of the proposed cloaking strategy could be investigated for a flexible scattering object. That said, these additional considerations will not be discussed further in this paper. The physical problem being considered here is unbounded, with the incident acoustic plane wave propagating from and to infinity, and therefore the Boundary Element Method was selected over the Finite Element Method [28, 29] as it does not require a large volumetric domain to be meshed [30] and bounded by a Perfectly Matched Layer [31], for example. Instead, only the surface of the scattering body requires a mesh, which results in a significant computational advantage. The model was meshed using free tetrahedral elements over the spherical scattering body with a minimum of 6 elements per acoustic wavelength. A convergence study was conducted, which confirmed that this mesh density is sufficient for consistent results [32].

The IRIDIS High Performance Computing Facility at the University of Southampton was used to solve the model described above over a range of frequencies between 100 Hz and 500 Hz. In each case, the

pressure due to the primary plane wave was calculated at each sensor location and these pressures were then used to form a vector of disturbance signals. The pressure contribution from each control source was also calculated at each sensor location by disabling the primary disturbance and driving each control source individually. This was then used to form the matrix of plant responses between the control sources and the far-field pressure sensors, $\mathbf{G_{ff}}$, and the matrix of plant responses between the control sources and the near-field pressure sensors,$\mathbf{G_{nf}}$. These matrices, as well as the vector of primary disturbance signals, will be used to assess the performance of the two proposed active control strategies in the next section.

3. FORMULATION

In this section, optimal control source strengths will be formulated for two separate control strategies: direct control of the scattered acoustic field, and quiet-zone control. These optimal formulations will then be combined with the simulation data, described in Section 2, to compare the two strategies. Both control strategies will be based on an optimal harmonic feedforward architecture, and in each case the vector of optimal source strengths will be expressed as $\mathbf{u}$, and the two matrices of complex plant response, $\mathbf{G_{ff}}$ and $\mathbf{G_{nf}}$, described in Section 2 will be used. The following formulations will be conducted in the frequency domain, however, the frequency dependence $e^{j\omega}$ will be omitted for notational convenience.

A. DIRECT SCATTERING CONTROL

In its most straightforward form, the scattering from an object can be controlled by directly minimising the vector of acoustic scattered pressures measured at a number of sensor locations in the far-field, $\mathbf{d_{s_{ff}}}$, using an array of control sources in the near-field of the scattering object. The vector of scattered acoustic pressures is given as

$$\mathbf{d_{s_{ff}}} = \mathbf{d_{t_{ff}}} - \mathbf{d_{i_{ff}}}, \tag{1}$$

where $\mathbf{d_{i_{ff}}}$ and $\mathbf{d_{t_{ff}}}$ are the vectors of incident acoustic pressures and total acoustic pressures respectively, measured at the far-field sensor array. The vector of scattered acoustic pressures after control, $\mathbf{e_{s_{ff}}}$, can be calculated at each sensor location as

$$\mathbf{e_{s_{ff}}} = \mathbf{d_{s_{ff}}} + \mathbf{G_{ff}}\mathbf{u}. \tag{2}$$

In the context of active acoustic cloaking, the controller aims to minimise the cost function J [33], given as

$$J = \mathrm{E}\left[{\mathbf{e_{s_{ff}}}}^H \mathbf{e_{s_{ff}}}\right], \tag{3}$$

where E is the expectation operator. By combining Equations 2 and 3, the cost function can be written as

$$J = \mathrm{E}\left[\left(\mathbf{d_{s_{ff}}} + \mathbf{G_{ff}}\mathbf{u}\right)^H \left(\mathbf{d_{s_{ff}}} + \mathbf{G_{ff}}\mathbf{u}\right)\right]. \tag{4}$$

By differentiating Equation 4 with respect to the real and imaginary parts of the matrix of control filter coefficients, and setting the real and imaginary parts to 0 as outlined in [34], the optimal set of control source strengths, $\mathbf{u_{opt}}$, is given as

$$\mathbf{u_{opt}} = -\left[{\mathbf{G_{ff}}}^H \mathbf{G_{ff}} + \beta\mathbf{I}\right]^{-1} {\mathbf{G_{ff}}}^H \mathbf{d_{s_{ff}}}, \tag{5}$$

where $\beta\mathbf{I}$ is a Tikhonov regularisation term [35], included to constrain the source strengths and reduce the effects of ill-conditioning on the matrix inversion.

B. QUIET-ZONE CONTROL

An alternative approach to actively cloaking a scattering object is to generate a zone of quiet around that object. The formulation for the optimal set of control sources in this case will be derived in this section.

The quiet-zone control strategy aims minimise the total acoustic pressure at a number of near-field sensors, which define the quiet-zone, whilst enforcing a minimum radiation condition on the control sources to limit their influence on the far-field pressures. The total acoustic pressure in the quiet-zone before control, $\mathbf{d_{t_{nf}}}$, is comprised of the incident and scattered components as

$$\mathbf{d_{t_{nf}}} = \mathbf{d_{i_{nf}}} + \mathbf{d_{s_{nf}}}, \tag{6}$$

where $\mathbf{d_{i_{nf}}}$ and $\mathbf{d_{s_{nf}}}$ are the vectors of incident acoustic pressures and scattered acoustic pressures respectively, measured at the near-field sensor array. The total acoustic pressure in the quiet-zone after control, $\mathbf{e_{t_{nf}}}$, can be calculated at the near-field sensor array as

$$\mathbf{e_{t_{nf}}} = \mathbf{d_{t_{nf}}} + \mathbf{G_{nf}}\mathbf{u}, \tag{7}$$

and the far-field radiated pressure from the control sources, $\mathbf{y_{c_{ff}}}$ is given as

$$\mathbf{y_{c_{ff}}} = \mathbf{G_{ff}}\mathbf{u}. \tag{8}$$

In the case of this constrained optimisation, the cost function to be minimised can be expressed as [36]

$$J = \mathrm{E}\left[\left(\mathbf{e_{t_{ff}}}^H \mathbf{e_{t_{ff}}}\right) + \lambda\left(\mathbf{y_{c_{ff}}}^H \mathbf{y_{c_{ff}}}\right)\right], \tag{9}$$

where λ is a weighting term that enables a trade-off between the relative importance of each of the cost function requirements. By combining Equations 7, 8 and 9, the cost function for the controller to minimise can be given as

$$J = \mathrm{E}\left[\left(\mathbf{d_{t_{nf}}} + \mathbf{G_{nf}}\mathbf{u}\right)^H \left(\mathbf{d_{t_{nf}}} + \mathbf{G_{nf}}\mathbf{u}\right) + \lambda\left(\mathbf{G_{ff}}\mathbf{u}\right)^H \left(\mathbf{G_{ff}}\mathbf{u}\right)\right]. \tag{10}$$

As in the previous section, the set of optimal source strengths that minimise this cost function can be calculated by differentiating and setting the real and imaginary parts to 0, which gives

$$\mathbf{u_{opt}} = -\left[\mathbf{G_{nf}}^H \mathbf{G_{nf}} + \lambda \mathbf{G_{ff}}^{\mathbf{H}} \mathbf{G_{ff}} + \beta \mathbf{I}\right]^{-1} \mathbf{G_{nf}}^H \mathbf{d_{t_{nf}}}, \tag{11}$$

where $\beta\mathbf{I}$ is a regularisation term as discussed previously.

4. ACOUSTIC CLOAKING PERFORMANCE

In the following analysis, the simulated data described in Section 2 will be used to investigate and compare the performance limitations of the two control strategies presented in Section 3. The regularisation terms in each case, β, and the constraint weighting term, λ, have been selected so as to ensure that the quiet-zone control approach achieves the greatest possible level of attenuation in the back-scattered pressure over an 8 m $\times$ 8 m plane. The direct-minimisation approach has been regularised to achieve the same frequency-averaged level of attenuation in the back-scattered pressure, thus aiming to provide a reasonable comparison between the two methods.

To ensure that the quiet-zone is performing as expected, the acoustic response within the quiet-zone will first be investigated. The total acoustic potential energy within the quiet-zone can be approximated by the sum of the squared pressures measured in the near-field zone. This has been calculated using the response from the near-field sensor array to approximate the total acoustic potential energy within the quiet-zone without active control, and with each of the two proposed control strategies formulated above. It should be highlighted that the direct-minimisation strategy has no consideration of the near-field total acoustic pressure, but it is still insightful to evaluate this performance metric. The resulting sum of the squared pressures in the quiet-zone for each control strategy are presented in Figure 2 and these results show that

the quiet-zone cloaking method achieves approximately 65 dB of attenuation within the quiet-zone, and this gradually reduces at frequencies above 375 Hz, so that the attenuation is around 35 dB at 500 Hz. This performance degradation is caused by spatial aliasing of the control source array, and corresponds to the frequency at which the arc-length between each control source is equal to half an acoustic wavelength. Figure 2 also shows that the direct-minimisation control method has little effect in the quiet-zone. This provides insight into the operation of the direct scattering control approach and how it differs from the quiet-zone method.

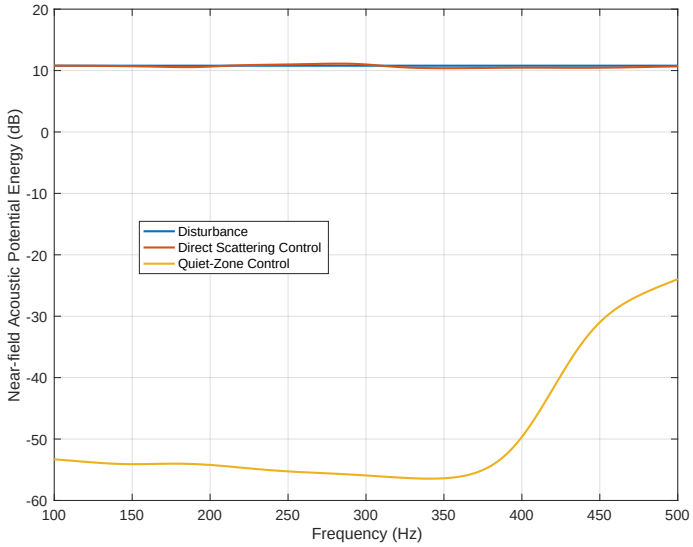

Figure 2: The acoustic potential energy in the quiet-zone estimated before control, and with each of the two control strategies.

The acoustic power due to a source of sound, W, can be approximated in the far-field by summing the squared response over N pressure sensors within the generated soundfield, as [37]

$$W = \sum_{l=1}^{N} \frac{|p_l^2|}{2\rho_0 c_0}, \tag{12}$$

where p_l is the acoustic pressure at the l-th sensor, ρ_0 is the density of the acoustic medium, and c_0 is the speed of sound. Equation 12 has been used to calculate the far-field scattered acoustic power, using the vector of scattered pressure measurements at the far-field sensor array. As with Figure 2, this has been calculated without active control, and with each of the proposed control strategies, and the results are presented in Figure 3. The scattered acoustic power before control is consistent with similar results in the literature showing the acoustic scattering from a sphere [12, 38, 39, 40]. Figure 3 shows that both control strategies are able to achieve an attenuation in the far-field scattered acoustic power across the presented frequency range, and the broadband average attenuation of the far-field scattered acoustic power for the quiet-zone cloaking strategy has been calculated to be 10.1 dB, whilst the broadband average for the direct-minimisation cloaking strategy has been calculated to be 16.9 dB. The performance of the quiet-zone method is reduced above approximately 400 Hz, corresponding to the frequency at which the control spacing is equal to half a wavelength, as discussed above.

Whilst the results presented above demonstrate that both acoustic cloaking methods are capable of achieving results at specific sensor locations, it is insightful to observe how the two control strategies influence the global sound-field. This will ensure that the control strategies are not only achieving local control at the error sensor locations, but producing a global effect. The optimal control sources calculated using Equations 5 and 11 have been implemented within the numerical model, which has subsequently been re-meshed and solved to observe the global effect of both cloaking strategies. Figure 4 shows the scattered

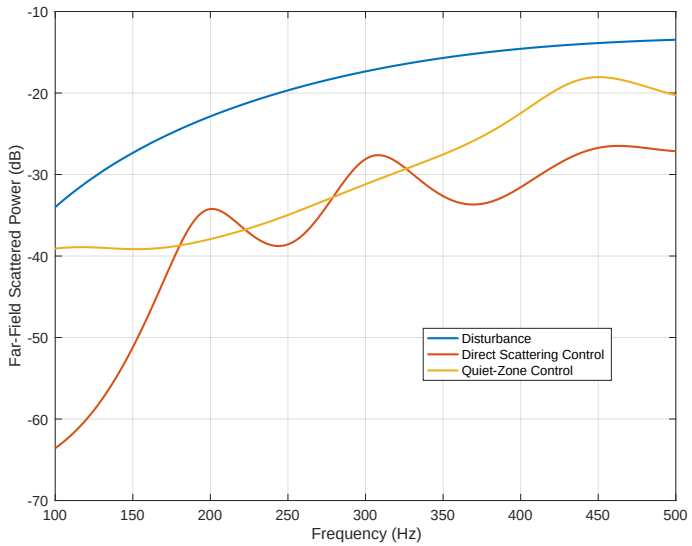

Figure 3: The far-field scattered acoustic power before control, and with each of the two control strategies.

pressure field at 300 Hz over an 8 m $\times$ 8 m grid for the uncontrolled case, and for each of the control strategies with the incident plane wave propagating upwards from the bottom of the frame. It can be seen from the results presented in Figure 4 that the direct-minimisation method is able to achieve a global attenuation in the acoustic scattered field, whilst the quiet-zone method is only able to achieve control of the back-scattered pressure. As the quiet-zone control method cancels the incident acoustic wave around the scattering object, the incident wave does not propagate down-stream and the quiet-zone control method does not attempt to actively reproduce the incident field down-stream of the scatterer in order to reduce the shadow-zone. For this reason, the quiet-zone cloaking method has the effect of significantly increasing the shadow-zone, and therefore increasing the level of acoustic scattering in the down-stream direction.

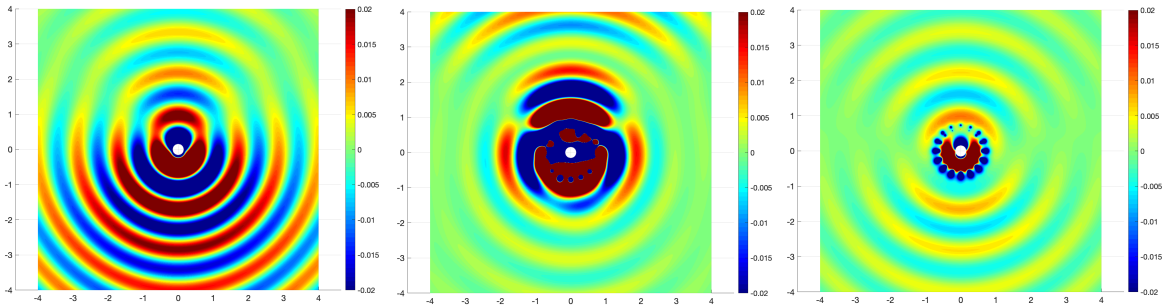

(a) Uncontrolled (b) Quiet-Zone Method (c) Direct-minimisation Method

Figure 4: Contour plots showing the scattered acoustic pressure field at 300 Hz for each control strategy

From the above results it has been shown that although direct-scattering control method generates a more effective cloaking system than the quiet-zone control method, the quiet-zone control method does achieve a significant level of scattering attenuation and may be more practicable. However, in a practical scenario it is also important to consider the control-effort, calculated as $\mathbf{u}^H\mathbf{u}$, required for each control strategy. This has been calculated and is presented in Figure 5 over frequency. These results show that despite the two control methods achieving similar levels of attenuation in the back-scattered acoustic pressure, and the direct-minimisation method also achieving a significant reduction in the shadow-zone scattering, the control-effort required by the quiet-zone cloaking strategy is approximately 30 dB greater than that for the direct-minimisation method. This can be explained by considering the relative levels of the incident and scattered fields, which can be evaluated based on the results presented in Figures 2

and 3 respectively. From these results it is clear that the incident field is of the order of 30 dB greater in level than the scattered field. Therefore, since the quiet-zone method attempts to control the incident field within the near-field region, it requires a significantly greater control effort than the direct-scattering control approach. It is worth noting that the performance of any practical system will be limited by the maximum power output of the control sources, and it should be ensured that the required control effort is within the linear operating range of the control sources.

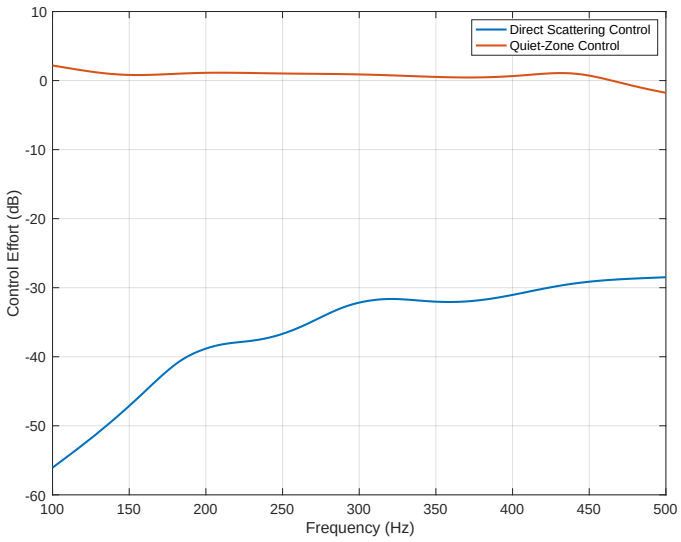

Figure 5: The control effort required by the two cloaking control strategies.

5. CONCLUSIONS

This paper has built on previous research that has proposed and investigated the use of an actively generated acoustic quiet-zone as an acoustic cloaking system. Whilst previous work has utilised high-order multipole acoustic sources or continuous distributions of monopoles and dipoles as the control sources, this paper has assumed a realistic arrangement of near-field and far-field pressure sensors, and a dual-layer array of monopole control sources. The performance limitations of the proposed quiet-zone control strategy have been compared to those for a direct-control approach using simulated data corresponding to a rigid sphere subject to an incident acoustic plane wave. The complex transfer responses between a number of monopole control sources and both near and far-field error sensors have been calculated. Optimal control source strengths for both the quiet-zone control method and the direct-scattering control method have been formulated, and the effect of regularisation has been discussed. It was found that the direct-minimisation control approach was able to achieve global control of the scattered field, whilst the quiet-zone method was only able to achieve control of the back-scattered pressure and the presence of the quiet-zone actually enhanced the shadow-zone. The control effort required for both methods was considered, and it was shown that the quiet-zone cloaking method requires significantly greater levels of control effort than the direct-minimisation approach.

Despite the potential disadvantages of the quiet-zone cloaking method discussed above, it should not be dismissed as a feasible control strategy. The main benefit of using the quiet-zone approach over direct-control of the scattered field is that the quiet-zone method requires no knowledge of the scattered acoustic pressure, nor does it require knowledge of the scattering object. This is a significant advantage, as a practical implementation of the direct-control cloaking system is currently not possible due to the requirement of a real-time measure of the acoustic scattered pressure. This study has shown that the

quiet-zone cloaking method is able to achieve considerable attenuation in the back-scattered pressure with a realistic arrangement of sensors and control sources, and this may enable a practical cloak provided that the down-stream scattered pressure is not of concern for the given application.

ACKNOWLEDGMENTS

This research was partially supported by an EPRSC iCASE studentship (Voucher number 16000059) and an EPSRC Prosperity Partnership (EP/S03661X/1). The authors acknowledge the use of the IRIDIS High Performance Computing Facility, and associated support services at the University of Southampton, in the completion of this work. The authors acknowledge the support from Professor William Parnell at the University of Manchester, whose insightful discussions helped to direct this research.

REFERENCES

[1] Marco Rahm, David Schurig, Daniel A. Roberts, Steven A. Cummer, David R. Smith, and John B. Pendry. Design of electromagnetic cloaks and concentrators using form-invariant coordinate transformations of Maxwell's equations. *Photonics and Nanostructures - Fundamentals and Applications*, 6(1):87–95, 2008.

[2] Liang Wu Cai and José Sánchez-Dehesa. Analysis of Cummer-Schurig acoustic cloaking. *New Journal of Physics*, 9, 2007.

[3] A. N. Norris and W. J. Parnell. Hyperelastic cloaking theory: transformation elasticity with pre-stressed solids. *Proceedings of the Royal Society A: Mathematical, Physical and Engineering Sciences*, 468(2146):2881–2903, 2012.

[4] Ying Cheng, Fan Yang, Jian Yi Xu, and Xiao Jun Liu. A multilayer structured acoustic cloak with homogeneous isotropic materials. *Applied Physics Letters*, 92(15), 2008.

[5] Matthew Reynolds, Yan Gao, and Steve Daley. Experimental validation of the band-gap and dispersive bulk modulus behaviour of locally resonant acoustic metamaterials. *Acoustical Society of America*, 19, 2013.

[6] Cecilia Casarini, James F.C. Windmill, and Joseph C. Jackson. 3D printed small-scale acoustic metamaterials based on Helmholtz resonators with tuned overtones. *Proceedings of IEEE Sensors*, 2017-Decem:1–3, 2017.

[7] Shu Zhang, Chunguang Xia, and Nicholas Fang. Broadband acoustic cloak for ultrasound waves. *Physical Review Letters*, 106(2):1–4, 2011.

[8] Lucian Zigoneanu, Bogdan Ioan Popa, and Steven A. Cummer. Three-dimensional broadband omnidirectional acoustic ground cloak. *Nature Materials*, 13(4):352–355, 2014.

[9] K. T. Tan, H. H. Huang, and C. T. Sun. Optimizing the band gap of effective mass negativity in acoustic metamaterials. *Applied Physics Letters*, 101(24), 2012.

[10] Emmanuel Friot, Régine Guillermin, and Muriel Winninger. Active control of scattered acoustic radiation: A real-time implementation for a three-dimensional object. *Acta Acustica united with Acustica*, 92(2):278–288, 2006.

[11] Seyyed M. Hasheminejad and M. Rajabi. Scattering and active acoustic control from a submerged piezoelectric-coupled orthotropic hollow cylinder. *Journal of Sound and Vibration*, 318(1-2):50–73, 2008.

[12] Jordan Cheer. Active control of scattered acoustic fields: Cancellation, reproduction and cloaking. *The Journal of the Acoustical Society of America*, 140(3):1502–1512, 2016.

[13] M. Rajabi and A. Mojahed. Active acoustic cloaking spherical shells. *Acta Acustica united with Acustica*, 104(1):5–12, 2018.

[14] Charlie House, Jordan Cheer, and Steve Daley. On the use of Virtual Sensing for the Real-Time Detection and Active Control of a Scattered Acoustic Field. In *International Congress on Sound & Vibration*, number 1, pages 1–8, 2019.

[15] C. Testa and L. Greco. Prediction of submarine scattered noise by the acoustic analogy. *Journal of Sound and Vibration*, 426:186–218, 2018.

[16] Ilkka Karasalo. Modelling of acoustic scattering from a submarine. *Proceedings of meetings on acoustics Acoustical Society of America*, (January):070017, 2012.

[17] Emmanuel Friot and C. Bordier. Real-time active suppression of scattered acoustic radiation. *Journal of Sound and Vibration*, 278(3):563–580, 2004.

[18] Fernando Guevara Vasquez, Graeme W. Milton, and Daniel Onofrei. Active exterior cloaking for the 2D Laplace and Helmholtz equations. *Physical Review Letters*, 103(7), 2009.

[19] Fernando Guevara Vasquez, Graeme W Milton, and Daniel Onofrei. Broadband exterior cloaking. *Optical Society of America*, 17(17):568–571, 2009.

[20] Thierry A. Beauvilain, J. Stuart Bolton, and Bryce K. Gardner. Sound cancellation by the use of secondary multipoles: Experiments. *The Journal of the Acoustical Society of America*, 107(3):1189–1202, 2002.

[21] Andrew N. Norris, Feruza A. Amirkulova, and William J. Parnell. Source amplitudes for active exterior cloaking. *Inverse Problems*, 28(10), 2012.

[22] Andrew N Norris and Feruza A Amirkulova. Active elastodynamic cloaking. *Mathematics and Mechanics of Solids*, 19(6):603–625, 2014.

[23] Fernando Guevara Vasquez, Graeme W. Milton, and Daniel Onofrei. Exterior cloaking with active sources in two dimensional acoustics. *Wave Motion*, 2011.
[24] Fernando Guevara Vasquez, Graeme W Milton, and Daniel Onofrei. Exterior cloaking with active sources in two dimensional acoustics. *Wave Motion*, 48(6):515–524, 2011.
[25] Fernando Guevara Vasquez, Graeme W Milton, and Daniel Onofrei. Mathematical analysis of the two dimensional active exterior cloaking in the quasistatic regime. *Analysis and Mathematical Physics*, 2012.
[26] Gregory Futhazar, William J. Parnell, and Andrew N. Norris. Active cloaking of flexural waves in thin plates. *Journal of Sound and Vibration*, 356:1–19, 2015.
[27] William B Gordon. Far-Field Approximations to the Kirchoff-Helmholtz Representations of Scattered Fields. *IEEE Transactions on Antennas and Propagation*, 53(1):590–592, 1975.
[28] Yunn Shiuan Liao, Shiang Woei Chyuan, and Jeng Tzong Chen. FEM versus BEM. *IEEE Circuits and Devices Magazine*, 20(5):25–34, 2004.
[29] Denny Fritze, Steffen Marburg, and Hans Jürgen Hardtke. FEM-BEM-coupling and structural-acoustic sensitivity analysis for shell geometries. *Computers and Structures*, 83(2-3):143–154, 2005.
[30] Soares Jr Delfim. Acoustic Modelling by BEM-FEM Coupling Procedures Taking into Account Explicit and Implicit Multi-Domain Decomposition Techniques. *International Journal for Numerical Methods in Engineering*, (February):1885–1891, 2009.
[31] Qing-Huo Liu and Jianping Tao. The perfectly matched layer for acoustic waves in absorptive media. *The Journal of the Acoustical Society of America*, 102(4):2072–2082, 2002.
[32] J.J do Rego Silva. *Acoustic and Elastic Wave Scattering using Boundary Elements*. WIT Press, 1994.
[33] C. R. Fuller, S. J. Elliott, and P. A. Nelson. Active Control of Vibration. In *Academic Press*. Academic Press, 1997.
[34] Stephen J. Elliott. *Signal Processing for Active Control*. Academic Press, 2001.
[35] Gene H Golub, Per Christian Hansen, and Dianne P O'Leary. Tikhonov Regularization and Total Least Squares. *Society for Industrial and Applied Mathematics Journal on Matrix Analysis and Applications*, 1999.
[36] P.A. Nelson and S.J. Elliott. *Active Control of Sound*. Academic Press, London, 1991.
[37] Lawrence E Kinsler and Austin R Frey. *Fundamentals of Acoustics*. John Wiley & Sons, 4th editio edition, 2000.
[38] Yu. I. Bobrovnitskii. A new impedance-based approach to analysis and control of sound scattering. *Journal of Sound and Vibration*, 297(3-5):743–760, 2006.
[39] Ning Han, Xiaojun Qiu, and Shengzhen Feng. Active control of three-dimension impulsive scattered radiation based on a prediction method. *Mechanical Systems and Signal Processing*, 30:267–273, 2012.
[40] Clyde Scandrett. Scattering and active acoustic control from a submerged spherical shell. *The Journal of the Acoustical Society of America*, 111(2):893, 2002.